Topics in Catalysis (2023) 66:1120–1128
https://doi.org/10.1007/s11244-023-01802-x

ORIGINAL PAPER

Water Splitting on a Pt_1/C_3N_4 Single Atom Catalyst: A Modeling Approach

Clara Saetta[1] · Giovanni Di Liberto[1] · Gianfranco Pacchioni[1]

Accepted: 2 March 2023 / Published online: 21 March 2023

Abstract
In this work we present a computational study of the nature of a Single Atom Catalyst (SAC) consisting of a Pt_1 atom anchored on a C_3N_4 support, and of its reactivity in the water splitting semi-reactions, the Hydrogen Evolution (HER) and Oxygen Evolution (OER) Reactions. The work is motivated by the intense research in designing catalytic materials for water splitting characterized by a low amount of noble metal species, maximization of active phase, and stability of the catalyst. C_3N_4-based SACs are promising candidates. The results indicate that the chemistry of a single atom is complex, as it can be anchored to the support in different ways resulting in a different stability. The reactivity of the most stable structure in HER and OER has been considered, finding that $Pt_1@C_3N_4$ is more reactive than metallic platinum. Furthermore, unconventional but stable intermediates can form that differ from the intermediates usually found on extended catalytic surfaces. The work highlights the importance of considering the complex chemistry of SACs in view of the analogies existing with coordination chemistry compounds.

Keywords DFT · SAC · C_3N_4 · HER · OER

1 Introduction

Converting water into molecular hydrogen and oxygen via a water splitting process stimulated by light (photocatalysis) or electricity (electrocatalysis) is one major challenge in the general frame of the energy transition, since the process provides a valuable fuel (and chemical), that can be used without emissions of greenhouse gases.[1–4] Unfortunately, the thermodynamic cost of the process is rather high. The reaction $2H_2O \rightarrow 2H_2 + O_2$ is an uphill process with a Gibbs free energy of 4.92 eV, which in real experiments is even higher due to overpotentials.

Among the best catalysts for this reaction are noble metals, such as Pd and Pt. The latter shows a nearly zero overpotential for the Hydrogen Evolution Reaction (HER)[5] and a value of about 0.4 eV for the Oxygen Evolution Reaction (OER).[6] The need to reduce the amount of noble metal loading or to replace it with other earth-abundant elements, as well as the need to improve the catalytic performances of existing catalysts has triggered an intense research activity aimed to design a new generation of catalytic materials.[7–12].

In the last few years, Single-Atom Catalysts (SACs) gained an increasing attention in the catalysis community. SACs are paradigmatic of single-site dispersion of metal species on a support, allowing in principle to maximize the active surface and therefore requiring a lower metal loading.[13–19] Furthermore, the activity of SACs can be substantially different from that of extended metals, opening in principle the possibility to optimize the catalysts through a rational design of the metal species and their local coordination.[20–25].

The chemical nature of SACs is inherently atomistic and hard to access based exclusively on experimental measurement. First principles simulations can be helpful to identify the structural geometry of SACs, their stability and activity, and in general for understanding their behavior. In this respect, theoretical models can assist and complement the experimental design of new active materials.

Transition metal atoms can bind in many different ways to the support that can be an oxide, a metal, a carbon-based nanomaterial, a sulfide, etc. The nature of the coordination is essential, since this largely affects the stability and

✉ Gianfranco Pacchioni
gianfranco.pacchioni@unimib.it

[1] Dipartimento di Scienza dei Materiali, Università di Milano-Bicocca, via Cozzi 55, 20125 Milano, Italy

resistance against sintering hence deactivation of the SAC. [26] And of course, the way the metal binds to the support determines its charge state, electronic configuration, and its reactivity in water splitting. Another interesting aspect is that SACs can be considered analogs of coordination chemistry compounds,[27–31] implying that HER and OER can occur via the formation of very stable intermediates that usually do not form on extended metal electrodes.[32–34] The description of all these aspects is essential to provide a fundamental understanding of the catalysts activity and eventually to provide reliable predictions about the reactivity of new catalysts.

In this work we investigate the complex nature and the properties of a specific SAC consisting of a Platinum atom embedded in a carbon nitride matrix and of its reactivity in the water splitting process.

The choice of the metal is motivated by the large interest in creating Pt-based catalysts for water splitting using small amounts of precious metals.[35, 36] The selection of the support is justified by the growing interest in carbon nitride for SACs,[37–39] given the capability of this material to stabilize single-site metal species. C_3N_4 has been used with promising results in a broad spectrum of catalytic reactions such as water splitting, but also CO_2 reduction, N_2 reduction, C-C coupling, and other relevant chemical processes. [37, 40–42].

The paper is organized as follows. Below we report the computational framework. Then we discuss the structure, stability and electronic properties of the $Pt_1@C_3N_4$ SAC focusing on the presence of several possible binding sites. Once the catalyst has been characterized, we will test it in HER and OER analyzing the possibility to form complexes in analogy to coordination chemistry compounds. Last, we will discuss the role played by solvation.

It is important to mention that the aim of the work is not that to predict how good or bad a specific catalyst is. Rather, we want to discuss some key ingredients that need to be included in the modeling of these systems. A reliable prediction of the catalytic activity in fact requires to address the experimental complexity, and to take into account effects such as solven, pH, applied voltage effects, [43–45]. Also, highly sophisticated but computationally expensive methods beyond DFT may be necessary in some cases.

2 Computational Details

We performed spin polarized DFT calculations as implemented in the VASP code.[46–48] The Perdew-Burke-Ernzerhof parametrization of the exchange and correlation functional was adopted [49]. The following valence electrons were treated explicitly: H (1s), C (2s,2p), N (2s, 2p), O (2s, 2p), Pt (6s, 5d). They have been expanded on a set of plane waves with a kinetic energy cutoff of 400 eV, whereas the core electrons were treated with the projector augmented wave approach (PAW).[50, 51] Dispersion forces have been included by the Grimme's D3 parameterization [52]. The threshold criteria for electronic and ionic loops were set to 10^{-5} eV and 10^{-2} eV/Å, respectively. It must be mentioned that the prediction of the electronic structure of the catalyst can be improved by adopting hybrid functionals, [53] that however are computationally more demanding. Since the goal of this work is not to provide absolute numbers of the activity but rather to investigate the complex chemistry of a SAC and its implications in HER and OER, we restrict the study to the level of PBE.

The support was modeled by considering a corrugated C_3N_4 nanosheet characterized by heptazine pores.[54] The optimized lattice parameters are $a = 13.846$ Å, $b = 6.923$ Å, $\gamma = 120°$ [40]. The sampling of the reciprocal space was done according to a (1×2) Monkhorst-Pack grid.[55].

The binding energy of the metal atom was calculated by taking as a reference the support and the free atom. The Gibbs free energy of chemical intermediates was evaluated by calculating the binding energy from DFT total energies (ΔE), and considering thermodynamic corrections by including entropic ($T\Delta S$), and zero-point energy contributions (ΔE_{ZPE}), as reported in Eq. 1 where n the number of electron-exchange involved and V is the applied voltage with respect to the Reversible Hydrogen Electrode (RHE), according to the seminal approach of Norskov and co-workers [56–58].

$$\Delta G(V) = \Delta E - T\Delta S + \Delta E_{ZPE} - nV \quad (1)$$

ΔS was calculated by taking gas-phase values from the literature and neglecting that of solid-state species. A possible way to improve the estimate is to evaluate the entropy of solid-state species through the formalism of the partition function within the harmonic approximation, although one should keep in mind that such approximation can be quite crude for vibrations involving hydrogen atoms. The neglection of the entropy contribution of solid-state species results in an error of the Gibbs free energies of about 0-1-0.2 eV. The zero-point energy contribution was estimated in a harmonic fashion, allowing the atoms of the chemical intermediate of interest and the metal atom to vibrate.[34] Table 1 reports the entropic and zero-point energy corrections. Relevant equations are reported in the SI.

3 Results and Discussion

3.1 Structure of Pt_1/C_3N_4 SAC

We started by anchoring the Pt atom on C_3N_4. We performed a global minimum search by starting geometry optimizations with the Pt atom on top of several N and C atoms, putting the Pt atom in bridge positions, and embedding the metal atom

Table 1 Entropic contribution at 298 K from international tables and calculated zero-point energies of various species. Values are in eV

eV	H_2	O_2	H_2O	OH*	O*	OOH*	OH*OH*	O*OH*	O_2*
$T\Delta S$	0.41	0.64	0.67	/	/	/	/	/	/
ΔE_{ZPE}	0.27	0.13	0.56	0.31	0.12	0.43	0.69	0.39	0.12

Table 2 Calculated relevant bond distances, binding energy of the metal, number of unpaired electrons, and atomic charge from the QTAIM.

Structure	$d_{M\text{-}N}$ / Å	$d_{M\text{-}C}$ / Å	ΔE_{ads} / eV	N° unpaired	q_{Pt} / |e|
Pore	2.05	/	− 2.97	0	0.41
	2.28				
	2.16				
Bridge	1.95	2.16	− 1.88	0	0.00
N_{top}	1.91	/	− 2.11	0	0.11

in the heptazine pore. The Pt atom can be embedded in the heptazine pore of the structure (Fig. 1a),[40] it can bind to C—N atoms and assume a bridge conformation (Fig. 1b), or it can go on-top of a nitrogen atom (Fig. 1c). In the first case the metal is coordinated to three nitrogen atoms with a bond-distance of about 2.1 Å. When Pt assumes a bridge position, the coordination number decreases to two, with $d_{Pt\text{-}N}$ 1.95 Å and $d_{Pt\text{-}C}$ 2.16 Å. In the last case, N_{top} configuration, Pt is coordinated to a single nitrogen atom with a calculated bond distance of 1.91 Å.

The global minimum structure is the pore site, while N_{top} and bridge have similar stabilities. The calculated bond-distances and adsorption energies are reported in Table 2.

We observe that the metal is rather stable when is embedded in the heptazine pore, as shown by the large negative binding energy (− 2.97 eV). The analysis of the metal magnetization indicates that in all cases there is no residual spin density on the metal. This information can be combined with the calculated atomic charge within the Quantum Theory of Atoms in Molecules (QTAIM), [59] see Table 2. Atomic

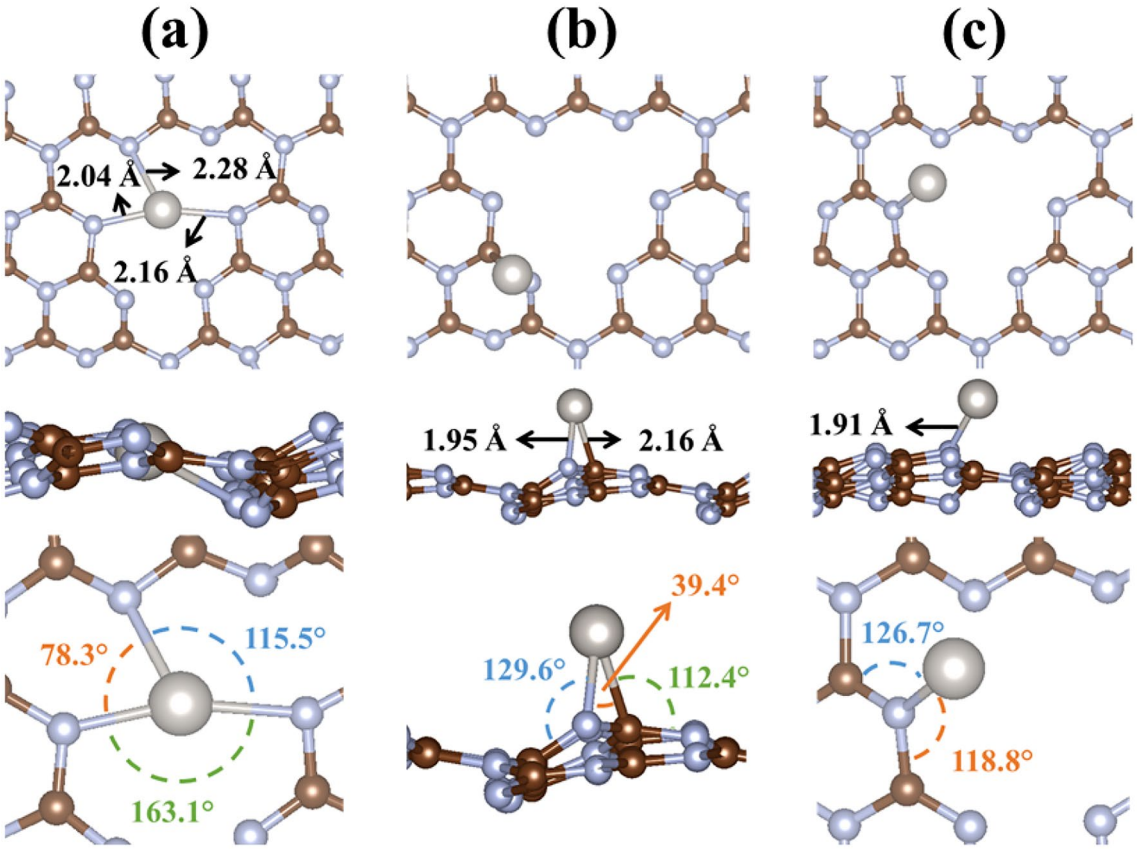

Fig. 1 Local coordination of Pt_1 species anchored on C_3N_4 assuming different configurations. From the left to right: **a** Pore, **b** Bridge and **c** N_{top} position

charges are not physical observable, and the results are strongly dependent on the partitioning criterion of the space in atomic basins.[60, 61] Therefore, absolute number must be taken with care. However, we can make some qualitative observation, in particular the stronger is the metal binding, the higher is the metal charge.

3.2 Reactivity in HER

We now investigate the reactivity of $Pt_1@C_3N_4$ in HER. We consider the global minimum structure, i.e. the metal atom embedded in the heptazine pore. Norskov and co-workers demonstrated that, on metals and oxide materials, the catalytic activity can be described by means of single descriptor, the Gibbs free energy of an adsorbed hydrogen atom.[56, 58, 62] This is based on the assumption that this species is the only reaction intermediate in the semi-reaction $H^+ + e^- \rightarrow ½\ H_2$. According to the Sabatier principle, the ideal catalyst corresponds to a system where the adsorption of the intermediate is thermoneutral with respect to the reference catalyst and the H_2 molecule. Both experimental and theoretical evidence indicate that the catalytic activity follows the Trasatti's volcano plot.[63].

SACs are analogs of coordination chemistry compounds. [27, 28] This can have sizeable implications on their catalytic activity in HER. In particular, the mechanism of the reaction of a single atom bound to a support can differ substantially from that of an extended metal surface. In this respect, we recently showed that dihydrogen and dihydride complexes can form on several SACs, showing that a new intermediate, HMH, can exists beside the classical MH one. When this is the case, it implies that the additional intermediate needs to be included in the kinetic modeling of the reaction.[32].

The case of $Pt_1@C_3N_4$ shows a clear example of the unique reactivity of SACs and the role of hydrogen complexes. The adsorption of the first hydrogen atom leads to a rather stable chemical intermediate (H*), $\Delta G = -0.60$ eV, and consequent large overpotential. The same process on metallic Pt has $\Delta G \sim 0.0$ eV, indicating that Pt_1 embedded in C_3N_4 binds hydrogen atoms much more strongly than metallic Pt. The adsorption of a second hydrogen atom leads to a very stable dihydride complex, $\Delta G = -1.37$ eV, see Fig. 2. The relevant bond distances and free energies are reported in Table 3. The H-H distance in the HMH complex (H_2*) is 1.98 Å, indicating a dihydride character.[32] Notice also that when the second H atom is bound to PtH the complex changes completely its geometrical structure, with the Pt atom leaving the pore of C_3N_4 and assuming a nearly square planar coordination, Fig. 2. It is interesting to observe that if we assume the same chemistry of the Pt SAC as for Pt metal, thus including in the modeling only the MH intermediate, one completely neglects the formation of the very stable HMH chemical species. This example further demonstrates the rich chemistry of SACs and the importance of accounting for the formation of intermediates that usually do not form on extended metal surfaces.

3.3 Reactivity in OER

The complex chemistry of SACs, and the need to include reaction intermediates that are usually not taken into account in the modeling of water splitting on metal electrodes becomes even more evident looking at the OER. The reaction is modeled on extended systems considering the formation of three key reaction intermediates, OH*, O*, and OOH*, according to the following chemical reactions, see also Fig. 3:

$$H_2O + {}^* \rightarrow OH^* + H^+ + e^- \quad (2)$$

$$OH^* \rightarrow O^* + H^+ + e^- \quad (3)$$

$$H_2O + O^* \rightarrow OOH^* + H^+ + e^- \quad (4)$$

$$OOH^* \rightarrow O_2 + {}^* + H^+ + e^- \quad (5)$$

The thermodynamic cost of this four-electron transfer process is 4.92 eV, therefore an ideal catalyst should bind all the intermediates with a free energy equal to zero assuming to apply a voltage $V = 1.23$ V vs. RHE. The calculated Gibbs free energy path is reported in Fig. 4. It should be mentioned at this point that the binding energy of O_2 molecule is significantly overestimated with the PBE functional. We used as a reference for the calculation of the free energies the bare catalyst and the experimental energy O_2 molecule.[34, 57, 64] More specifically, the experimental Gibbs free energy for the reaction $2H_2O \rightarrow O_2 + 4\ H^+ + 4e^-$ is 4.92 eV, and the corresponding Gibbs free energy of O_2 at $V = 1.23$ eV is equal to $\Delta G = 4.92\ \text{eV} - 4e^- \cdot 1.23\ \text{V} = 0.00$ eV, Fig. 4.

As we mentioned above, on SACs other intermediates can form. This is the case also of the OER, and we recently demonstrated that superoxo and peroxo species can form on SACs.[34] In general, the metal atom can increase its coordination by binding more than one oxygenate species, leading

Table 3 Calculated bond distances and Gibbs free energy of H* and H_2* intermediates

System	$d_{M\text{-}H}$ / Å	$d_{H\text{-}H}$ / Å	ΔG / eV
H*	1.55	/	−0.60
H_2*	1.56	1.98	−1.37
	1.57		

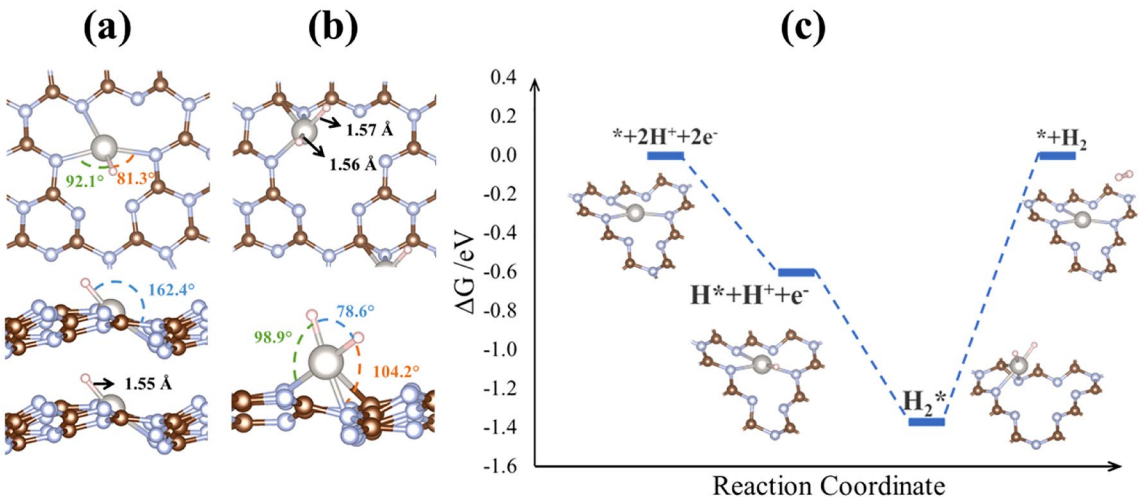

Fig. 2 Structure of H* **a** and H_2* **b** on Pt_1/C_3N_4 and the resulting Gibbs free energy profile **c** assuming to apply a voltage V = 0 V with respect to RHE. The reference is the bare catalyst and the H_2 molecule

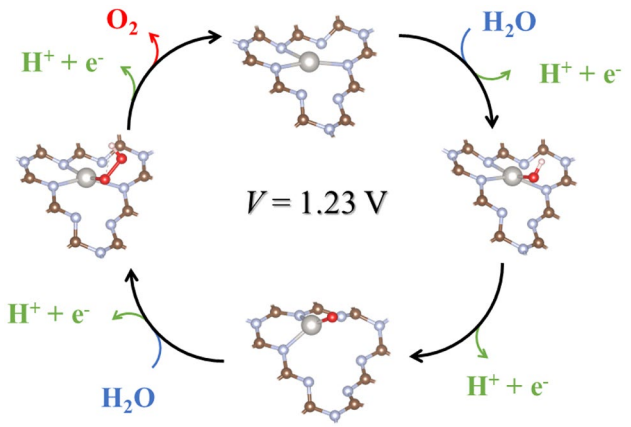

Fig. 3 Conventional OER reaction path on Pt_1/C_3N_4

to a series of unconventional chemical intermediates.[33, 34] For instance, after the adsorption of OH*, a second OH* can bind on the same site, forming a OH*OH* complex.[33] The formation of this species implies a total release of two electrons, as well as for the O* species.

$$2H_2O + * \rightarrow OH^*OH^* + 2H^+ + 2e^- \quad (6)$$

The reaction can proceed with the release of a third electron forming the O*OH* intermediate, a species which is competitive with OOH*:

$$2H_2O + * \rightarrow O^*OH^* + 3H^+ + 3e^- \quad (7)$$

The release of another electron can give raise to the formation of a peroxo or superoxo complex, O_2*:

$$2H_2O + * \rightarrow O_2^* + 4H^+ + 4e^- \quad (8)$$

that finally can release molecular oxygen to the gas-phase.

To show the importance of these intermediates, we reported the corresponding Gibbs free energy profile, Fig. 4, and we compared the resulting reaction path with that derived considering the classical OH*, O*, and OOH* intermediates only. We first observe that the SAC is once again more reactive than metallic platinum, forming stable intermediates. For instance, the calculated free energy of OH* is − 0.45 eV, to be compared with the same values at the same level of theory of metallic platinum, 0.97 eV [66]. Table 4 also reports the relevant bond distances and the calculated Gibbs free energies. Interestingly, the reactivity of $Pt_1@C_3N_4$ is high, and the unconventional intermediates are substantially more stable than the conventional ones. This result suggests that Pt_1/C_3N_4 prefers to form these unconventional complexes. Once again, the peculiar chemistry of SACs at variance with extended materials is apparent, as well as the importance of considering the formation of unconventional chemical intermediates.

These results imply that, at this level of modeling, $Pt_1@C_3N_4$ is not an ideal catalyst for OER, because of the very strong binding of some intermediates. As mentioned above, the purpose of this study is not to identify a potentially good catalyst for HER or OER, but rather to highlight the complex chemistry of SACs, the analogies with coordination chemistry, and how the behavior can substantially differ from that of extended metal surfaces.

Table 4 Calculated bond distances and Gibbs free energy of OER intermediates. The latter are reported assuming to apply a voltage V = 1.23 V vs. RHE.

System	$d_{M\text{-}O}$ / Å	$d_{O\text{-}O}$ / Å	ΔG / eV
OH*	0.98	/	−0.45
O*	1.77		−1.28
OOH*	1.99	1.46	0.27
OH*OH*	1.97	/	−2.09
	1.97		
O*OH*	1.83	/	−1.61
	1.97		
O_2*	1.99	1.39	−1.94
	1.99		

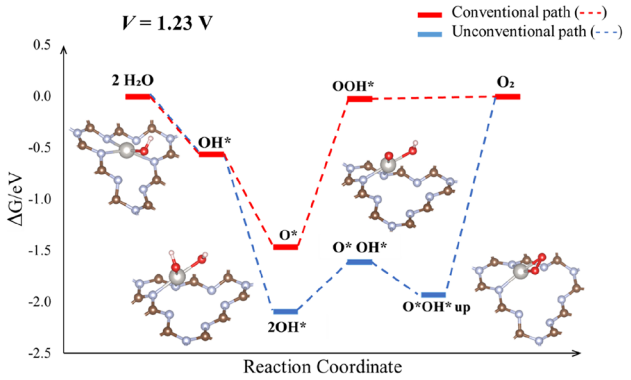

Fig. 4 Gibbs free energy profile of OER assuming the conventional path (red) and the unconventional one (light blue) assuming to apply a voltage V = 1.23 V vs. RHE. The reference experimental energy of O_2 molecule is used

3.4 Role of Solvation: Microsolvation Model

One relevant aspect when dealing with the reaction of water splitting is the role of solvation, since the reaction occurs in a liquid phase and the solvent (water in this case) can affect the stability of the intermediates and modify reaction free energy profiles. The treatment of solvent effects is challenging, since one must simulate solid/liquid interfaces and account for dynamical effects, for instance by making use of ab-initio molecular dynamics simulations.[65–68] Alternative approaches have been proposed such as the implicit solvent model,[70] or models where the water molecules are explicitly considered. One of these latter approaches approximates the solvation environment with a static framework of water molecules, often referred to as the water bilayer model, [69–71] However, also this approach is computationally rather demanding. Recently, Calle-Vallejo et al. proposed a much simpler approach, where the role of solvation is approximated by considering only a small solvation shell characterized by an optimum number of water molecules. This number was established to be equal to three.[72] According to some estimates, the method provides results comparable to those of the water bilayer model.

Here we considered the role of the solvent adopting this latter model, also called microsolvation model. The aim is to find if the solvent has a sizable effect on the stability of the various intermediates found in the reactions studied. We restrict the analysis to the OER, and we simulated the OER intermediates in the presence of three water molecules. The corresponding Gibbs free energy profiles have thus been determined. Figures S1 and S2 show the structure of the intermediates in the presence of water, where the formation of a local solvation environment held together by hydrogen bonding can be observed. These energy profiles are calculated as the difference between the free energy of the intermediate in the presence of water and the same profile obtained in vacuum condition. Not surprisingly, solvation stabilizes all the species. In particular, OH*, O*, and OOH* intermediates undergo a nearly systematic stabilization of about −0.3/−0.4 eV. This applies also to the unconventional intermediates, with the only exception of the OH*OH* complex where the stabilization is larger. The free energy profiles, Fig. 5, show that while solvation stabilize all species involved to a different extent, it does not alter the energetic ordering, which remains the same found with calculations done in vacuum conditions. Of course, one should be careful in generalizing this result to other reactions or other catalysts involved in OER.

One major problem when treating solvation is the presence of several local minima very close in energy.[73, 74] A second problem is the size of the coordination shell. It was recently demonstrated that one should consider a larger solvation shell of about 20 water molecules to properly reproduce a solvation environment.[75] For these reasons,

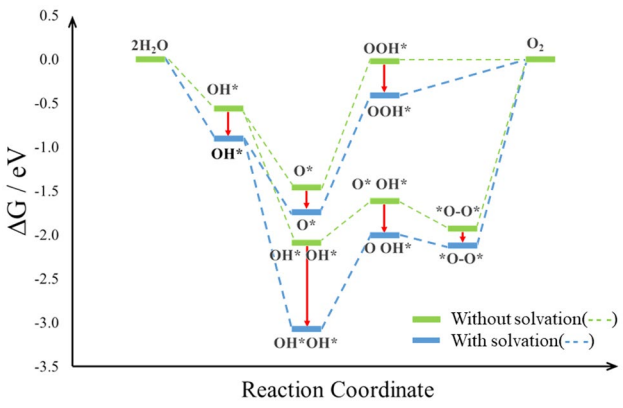

Fig. 5 OER conventional and unconventional Gibbs free energy profiles (V = 1.23 V) in vacuum conditions (green) and including solvation according to the microsolvation approach (light blue)

a quantitative estimate of the role of solvation requires more elaborated approaches that should also include dynamical aspects.

4 Conclusions

In this work we presented a computational study of the activity of a Pt_1/C_3N_4 Single-Atom Catalyst in HER and OER by means of a Density Functional Theory approach. We first investigated the structure of the catalyst finding a complex picture where the metal can bind the catalyst in different ways. In particular, it can be anchored in the heptazine pore, it can occupy a bridge position between C and N atoms, or it can go on-top of N atoms. The pore structure is the global minimum, showing a significant binding energy close to -3 eV. This suggests that the system could be sufficiently stable to stay intact during the catalytic process.

This system was used for the investigation of the reactivity in HER and OER. When studying the first process, we found that the Pt atom is very reactive and binds hydrogen atoms more strongly than a Pt metal electrode. In addition, besides the classical MH intermediate where a single H atom is bound to the Pt catalytic center, we found that the formation of a stable dihydride complex is possible, providing a clear example of the analogy between SACs and coordination chemistry compounds. This result points to the importance of considering the formation unconventional species to properly account for the chemistry of SACs.

This aspect is even more relevant when looking at the OER. We simulated the conventional reaction path, based on the formation of OH*, O*, and OOH* intermediates, but we also considered the formation of other species where the Pt atom can coordinate two oxygenate species. The analysis of the free energy profile shows that the formation of these "unconventional" intermediates is clearly preferred leading to a completely different reaction mechanism. We also observed that the SAC forms very stable intermediates, implying large overpotentials. This result motivates further investigation on the activation of very stable molecules such as CO_2 and N_2.

Finally, we estimated the role of solvation by means of the microsolvation approach. We found that the effect of solvation is sizeable, since the solvent stabilizes all the species involved in the reaction, but that this does not alter the mechanism found with calculations done in vacuum.

The work provides a further proof of the peculiar reactivity of SACs when compared with extended metal surfaces, and it shows the crucial importance to explore the capability of SACs to form various complexes. Only if a full analysis of the possible intermediates is done a kinetic model can be built.

Supplementary Information The online version contains supplementary material available at https://doi.org/10.1007/s11244-023-01802-x.

Acknowledgements We thank Livia Giordano for useful discussions. We acknowledge the financial support from Cariplo foundation. Access to the CINECA supercomputing resources was granted via ISCRAB. We also thank the COST Action 18234 supported by COST (European Cooperation in Science and Technology).

Author Contributions The manuscript was written through contributions of all authors.

Funding Open access funding provided by Università degli Studi di Milano - Bicocca within the CRUI-CARE Agreement. Fondazione Cariplo,Carbon dioxide conversion into energy-rich molecules with tailored catalysts CO2ENRICH, Gianfranco Pacchioni, European Cooperation in Science and Technology,18234, Gianfranco Pacchioni

Declarations

Conflict of interest The authors declare no conflict of interest.

References

1. Christoforidis KC, Fornasiero P (2017) Photocatalytic hydrogen production: a rift into the Future Energy Supply. ChemCatChem 9:1523–1544. https://doi.org/10.1002/cctc.201601659
2. Walter MG, Warren EL, McKone JR et al (2010) Solar Water Splitting cells. Chem Rev 110:6446–6473. https://doi.org/10.1021/cr1002326
3. Chen S, Takata T, Domen K (2017) Particulate photocatalysts for overall water splitting. Nat Rev Mater 2:17050. https://doi.org/10.1038/natrevmats.2017.50
4. Samanta B, Morales-García Á, Illas F et al (2022) Challenges of modeling nanostructured materials for photocatalytic water splitting. Chem Soc Rev 51:3794–3818. https://doi.org/10.1039/D1CS00648G
5. Lindgren P, Kastlunger G, Peterson AA (2020) A challenge to the G ~ 0 interpretation of Hydrogen Evolution. ACS Catal 10:121–128. https://doi.org/10.1021/acscatal.9b02799
6. Heard DM, Lennox AJJ (2020) Electrode materials in Modern Organic Electrochemistry. Angew Chemie Int Ed 59:18866–18884. https://doi.org/10.1002/anie.202005745
7. Vesborg PCK, Jaramillo TF (2012) Addressing the terawatt challenge: scalability in the supply of chemical elements for renewable energy. RSC Adv 2:7933. https://doi.org/10.1039/c2ra20839c
8. Fei H, Dong J, Arellano-Jiménez MJ et al (2015) Atomic cobalt on nitrogen-doped graphene for hydrogen generation. Nat Commun 6:8668. https://doi.org/10.1038/ncomms9668

9. Abdi FF, Han L, Smets AHM et al (2013) Efficient solar water splitting by enhanced charge separation in a bismuth vanadate-silicon tandem photoelectrode. Nat Commun 4:2195:1–7. https://doi.org/10.1038/ncomms3195
10. Zou X, Zhang Y (2015) Noble metal-free hydrogen evolution catalysts for water splitting. Chem Soc Rev 44:5148–5180. https://doi.org/10.1039/C4CS00448E
11. Rao RR, Kolb MJ, Giordano L et al (2020) Operando identification of site-dependent water oxidation activity on ruthenium dioxide single-crystal surfaces. Nat Catal 3:516–525. https://doi.org/10.1038/s41929-020-0457-6
12. Gauthier JA, Dickens CF, Chen LD et al (2017) Solvation Effects for Oxygen Evolution reaction catalysis on IrO 2 (110). J Phys Chem C 121:11455–11463. https://doi.org/10.1021/acs.jpcc.7b02383
13. Wang A, Li J, Zhang T (2018) Heterogeneous single-atom catalysis. Nat Rev Chem 2:65–81. https://doi.org/10.1038/s41570-018-0010-1
14. Qiao B, Wang A, Yang X et al (2011) Single-atom catalysis of CO oxidation using Pt1/FeOx. Nat Chem 3:634–641. https://doi.org/10.1038/nchem.1095
15. Qiu H-J, Ito Y, Cong W et al (2015) Nanoporous graphene with single-atom nickel dopants: an efficient and stable Catalyst for Electrochemical Hydrogen production. Angew Chemie Int Ed 54:14031–14035. https://doi.org/10.1002/anie.201507381
16. Cheng N, Stambula S, Wang D et al (2016) Platinum single-atom and cluster catalysis of the hydrogen evolution reaction. Nat Commun 7:13638. https://doi.org/10.1038/ncomms13638
17. Liu J-C, Wang Y-G, Li J (2017) Toward Rational Design of Oxide-Supported single-atom catalysts: atomic dispersion of gold on Ceria. J Am Chem Soc 139:6190–6199. https://doi.org/10.1021/jacs.7b01602
18. Vilé G, Albani D, Nachtegaal M et al (2015) A stable single-site Palladium Catalyst for Hydrogenations. Angew Chemie Int Ed 54:11265–11269. https://doi.org/10.1002/anie.201505073
19. Chen Z, Vorobyeva E, Mitchell S et al (2018) A heterogeneous single-atom palladium catalyst surpassing homogeneous systems for Suzuki coupling. Nat Nanotechnol 13:702–707. https://doi.org/10.1038/s41565-018-0167-2
20. Hossain MD, Liu Z, Zhuang M et al (2019) Rational design of Graphene-Supported single atom catalysts for hydrogen evolution reaction. Adv Energy Mater 9:1803689. https://doi.org/10.1002/aenm.201803689
21. Huang H-C, Zhao Y, Wang J et al (2020) Rational design of an efficient descriptor for single-atom catalysts in the hydrogen evolution reaction. J Mater Chem A 8:9202–9208. https://doi.org/10.1039/D0TA01500H
22. Wu L, Guo T, Li T (2020) Rational design of transition metal single-atom electrocatalysts: a simulation-based, machine learning-accelerated study. J Mater Chem A 8:19290–19299. https://doi.org/10.1039/D0TA06207C
23. Di Liberto G, Cipriano LA, Pacchioni G (2022) Single Atom Catalysts: What Matters Most the Active Site or The Surrounding? ChemCatChem. https://doi.org/10.1002/cctc.202200611
24. Di Liberto G, Cipriano LA, Pacchioni G (2022) Universal Principles for the Rational design of single atom electrocatalysts? Handle with Care. ACS Catal. https://doi.org/10.1021/acscatal.2c01011
25. Tosoni S, Di Liberto G, Matanovic I, Pacchioni G (2023) Modelling single atom catalysts for water splitting and fuel cells: a tutorial review. J Power Sources 556:232492. https://doi.org/10.1016/j.jpowsour.2022.232492
26. DeRita L, Resasco J, Dai S et al (2019) Structural evolution of atomically dispersed pt catalysts dictates reactivity. Nat Mater 18:746–751. https://doi.org/10.1038/s41563-019-0349-9
27. Copéret C, Chabanas M, Petroff Saint-Arroman R, Basset J-M (2003) Homogeneous and heterogeneous catalysis: bridging the gap through Surface Organometallic Chemistry. Angew Chemie Int Ed 42:156–181. https://doi.org/10.1002/anie.200390072
28. Copéret C, Comas-Vives A, Conley MP et al (2016) Surface Organometallic and Coordination Chemistry toward single-site heterogeneous catalysts: strategies, methods, structures, and activities. Chem Rev 116:323–421. https://doi.org/10.1021/acs.chemrev.5b00373
29. Jakub Z, Hulva J, Meier M et al (2019) Local structure and coordination define adsorption in a model ir 1 /Fe 3 O 4 single-atom Catalyst. Angew Chemie 131:14099–14106. https://doi.org/10.1002/ange.201907536
30. Parkinson GS (2019) Single-atom catalysis: how structure influences Catalytic Performance. Catal Lett 149:1137–1146. https://doi.org/10.1007/s10562-019-02709-7
31. Di Liberto G, Tosoni S, Cipriano LA, Pacchioni G (2022) A few questions about single-atom catalysts: when modeling helps. Acc Mater Res 3:986–995. https://doi.org/10.1021/accountsmr.2c00118
32. Di Liberto G, Cipriano LA, Pacchioni G (2021) Role of Dihydride and Dihydrogen Complexes in Hydrogen Evolution reaction on single-atom catalysts. J Am Chem Soc 143:20431–20441. https://doi.org/10.1021/jacs.1c10470
33. Zhong L, Li S (2020) Unconventional oxygen reduction reaction mechanism and scaling relation on single-atom catalysts. ACS Catal 10:4313–4318. https://doi.org/10.1021/acscatal.0c00815
34. Cipriano LA, Di Liberto G, Pacchioni G (2022) Superoxo and Peroxo Complexes on single-atom catalysts: impact on the Oxygen Evolution reaction. ACS Catal. https://doi.org/10.1021/acscatal.2c03020
35. Zhang L, Long R, Zhang Y et al (2020) Direct Observation of dynamic bond evolution in single-atom Pt/C 3 N 4 catalysts. Angew Chemie 132:6283–6288. https://doi.org/10.1002/ange.201915774
36. Zhou P, Lv F, Li N et al (2019) Strengthening reactive metal-support interaction to stabilize high-density pt single atoms on electron-deficient g-C3N4 for boosting photocatalytic H2 production. Nano Energy 56:127–137. https://doi.org/10.1016/j.nanoen.2018.11.033
37. Mishra A, Mehta A, Basu S et al (2019) Graphitic carbon nitride (g–C3N4)–based metal-free photocatalysts for water splitting: a review. Carbon N Y 149:693–721. https://doi.org/10.1016/j.carbon.2019.04.104
38. Ong W-J, Tan L-L, Ng YH et al (2016) Graphitic Carbon Nitride (g-C 3 N 4)-Based photocatalysts for Artificial Photosynthesis and Environmental Remediation: are we a step closer to achieving sustainability? Chem Rev 116:7159–7329. https://doi.org/10.1021/acs.chemrev.6b00075
39. Zhao Z, Sun Y, Dong F (2015) Graphitic carbon nitride based nanocomposites: a review. Nanoscale 7:15–37. https://doi.org/10.1039/C4NR03008G
40. Vilé G, Di Liberto G, Tosoni S et al (2022) Azide-Alkyne click Chemistry over a heterogeneous copper-based single-atom Catalyst. ACS Catal 12:2947–2958. https://doi.org/10.1021/acscatal.1c05610
41. Chen Z, Zhao J, Cabrera CR, Chen Z (2019) Computational screening of efficient single-atom catalysts based on Graphitic Carbon Nitride (g-C3N4) for Nitrogen Electroreduction. Small Methods 3:1800368. https://doi.org/10.1002/smtd.201800368
42. Bajada MA, Sanjosé-Orduna J, Di Liberto G et al (2022) Interfacing single-atom catalysis with continuous-flow organic electrosynthesis. Chem Soc Rev 51:3898–3925. https://doi.org/10.1039/D2CS00100D
43. Cheng T, Wang L, Merinov BV, Goddard WA (2018) Explanation of dramatic pH-Dependence of hydrogen binding on Noble Metal

Electrode: greatly weakened Water Adsorption at High pH. J Am Chem Soc 140:7787–7790. https://doi.org/10.1021/jacs.8b04006
44. Rojas-Carbonell S, Artyushkova K, Serov A et al (2018) Effect of pH on the activity of Platinum Group Metal-Free catalysts in Oxygen reduction reaction. ACS Catal 8:3041–3053. https://doi.org/10.1021/acscatal.7b03991
45. Melander MM, Kuisma MJ, Christensen TEK, Honkala K (2019) Grand-canonical approach to density functional theory of electrocatalytic systems: thermodynamics of solid-liquid interfaces at constant ion and electrode potentials. J Chem Phys 150:041706. https://doi.org/10.1063/1.5047829
46. Kresse G, Hafner J (1993) Ab initio molecular dynamics for liquid metals. Phys Rev B 47:558–561. https://doi.org/10.1103/PhysRevB.47.558
47. Kresse G, Hafner J (1994) Ab initio molecular-dynamics simulation of the liquid-metal–amorphous-semiconductor transition in germanium. Phys Rev B 49:14251–14269. https://doi.org/10.1103/PhysRevB.49.14251
48. Kresse G, Furthmüller J (1996) Efficiency of ab-initio total energy calculations for metals and semiconductors using a plane-wave basis set. Comput Mater Sci 6:15–50. https://doi.org/10.1016/0927-0256(96)00008-0
49. Perdew JP, Burke K, Ernzerhof M (1996) Generalized gradient approximation made simple. Phys Rev Lett 77:3865–3868. https://doi.org/10.1103/PhysRevLett.77.3865
50. Kresse G, Joubert D (1999) From ultrasoft pseudopotentials to the projector augmented-wave method. Phys Rev B 59:1758–1775. https://doi.org/10.1103/PhysRevB.59.1758
51. Blöchl PE (1994) Projector augmented-wave method. Phys Rev B 50:17953–17979. https://doi.org/10.1103/PhysRevB.50.17953
52. Grimme S, Antony J, Ehrlich S, Krieg H (2010) A consistent and accurate ab initio parametrization of density functional dispersion correction (DFT-D) for the 94 elements H-Pu. J Chem Phys 132:154104. https://doi.org/10.1063/1.3382344
53. Barlocco I, Cipriano LA, Di Liberto G, Pacchioni G (2022) Modeling hydrogen and oxygen evolution reactions on single atom catalysts with density functional theory: role of the functional. Adv Theory Simul. https://doi.org/10.1002/adts.202200513
54. Di Liberto G, Tosoni S, Pacchioni G (2021) Z-Scheme versus type-II junction in g-C 3 N 4 /TiO 2 and g-C 3 N 4 /SrTiO 3 /TiO 2 heterostructures. Catal Sci Technol 11:3589–3598. https://doi.org/10.1039/D1CY00451D
55. Monkhorst HJ, Pack JD (1976) Special points for Brillouin-zone integrations. Phys Rev B 13:5188–5192. https://doi.org/10.1103/PhysRevB.13.5188
56. Nørskov JK, Bligaard T, Logadottir A et al (2005) Trends in the Exchange Current for Hydrogen Evolution. J Electrochem Soc 152:J23. https://doi.org/10.1149/1.1856988
57. Nørskov JK, Rossmeisl J, Logadottir A et al (2004) Origin of the Overpotential for Oxygen reduction at a fuel-cell cathode. J Phys Chem B 108:17886–17892. https://doi.org/10.1021/jp047349j
58. Nørskov JK, Bligaard T, Rossmeisl J, Christensen CH (2009) Towards the computational design of solid catalysts. Nat Chem 1:37–46. https://doi.org/10.1038/nchem.121
59. Bader RFW (1985) Atoms in molecules. Acc Chem Res 18:9–15. https://doi.org/10.1021/ar00109a003
60. Walsh A, Sokol AA, Buckeridge J et al (2017) Electron counting in solids: Oxidation States, partial charges, and ionicity. J Phys Chem Lett 8:2074–2075. https://doi.org/10.1021/acs.jpclett.7b00809
61. Walsh A, Sokol AA, Buckeridge J et al (2018) Oxidation states and ionicity. Nat Mater 17:958–964. https://doi.org/10.1038/s41563-018-0165-7
62. Norskov JK, Christensen CH (2006) Toward Efficient Hydrogen Production at Surfaces. Science 80(312):1322LP – 1323. https://doi.org/10.1126/science.1127180
63. Trasatti S (1972) Work function, electronegativity, and electrochemical behaviour of metals. J Electroanal Chem Interfacial Electrochem 39:163–184. https://doi.org/10.1016/S0022-0728(72)80485-6
64. Rossmeisl J, Qu Z-W, Zhu H et al (2007) Electrolysis of water on oxide surfaces. J Electroanal Chem 607:83–89. https://doi.org/10.1016/j.jelechem.2006.11.008
65. Di Liberto G, Giordano L (2023) Role of solvation model on the stability of oxygenates on pt(111): a comparison between microsolvation, extended bilayer, and extended metal/water interface. Electrochem Sci Adv. https://doi.org/10.1002/elsa.202100204
66. Ambrosio F, Wiktor J, Pasquarello A (2018) pH-Dependent Surface Chemistry from First Principles: application to the BiVO 4 (010)–Water interface. ACS Appl Mater Interfaces 10:10011–10021. https://doi.org/10.1021/acsami.7b16545
67. Ambrosio F, Guo Z, Pasquarello A (2018) Absolute energy levels of Liquid Water. J Phys Chem Lett 9:3212–3216. https://doi.org/10.1021/acs.jpclett.8b00891
68. Di Liberto G, Maleki F, Pacchioni G (2022) pH dependence of MgO, TiO 2, and γ-Al 2 O 3 Surface Chemistry from First Principles. J Phys Chem C 126:10216–10223. https://doi.org/10.1021/acs.jpcc.2c02289
69. Mennucci B (2012) Polarizable continuum model. WIREs Comput Mol Sci 2:386–404. https://doi.org/10.1002/wcms.1086
70. Feibelman PJ (2002) Partial dissociation of Water on Ru(0001). Sci (80-) 295:99–102. https://doi.org/10.1126/science.1065483
71. He Z-D, Hanselman S, Chen Y-X et al (2017) Importance of Solvation for the Accurate Prediction of Oxygen reduction activities of Pt-Based electrocatalysts. J Phys Chem Lett 8:2243–2246. https://doi.org/10.1021/acs.jpclett.7b01018
72. Calle-Vallejo F, de Morais F, Illas R F, et al (2019) Affordable estimation of Solvation Contributions to the Adsorption energies of oxygenates on metal nanoparticles. J Phys Chem C 123:5578–5582. https://doi.org/10.1021/acs.jpcc.9b01211
73. Keutsch FN, Saykally RJ (2001) Water clusters: untangling the mysteries of the liquid, one molecule at a time. Proc Natl Acad Sci 98:10533–10540. https://doi.org/10.1073/pnas.191266498
74. Di Liberto G, Conte R, Ceotto M (2018) Divide-and-conquer" semiclassical molecular dynamics: an application to water clusters. J Chem Phys 148:104302. https://doi.org/10.1063/1.5023155
75. Rognoni A, Conte R, Ceotto M (2021) How many water molecules are needed to solvate. one? Chem Sci 12:2060–2064. https://doi.org/10.1039/D0SC05785A